arXiv:1611.03359v1 [nucl-th] 10 Nov 2016

Formation of hypernuclei in evaporation and fission processes

A.S. Botvina[1,2], N. Buyukcizmeci[3], A. Ergun[3], R. Ogul[3], M. Bleicher[1], J. Pochodzalla[4]

[1]*Frankfurt Institute for Advanced Studies and ITP J.W. Goethe University, D-60438 Frankfurt am Main, Germany*

[2]*Institute for Nuclear Research, Russian Academy of Sciences, 117312 Moscow, Russia*

[3]*Department of Physics, Selcuk University, 42079 Kampus, Konya, Turkey and*

[4] *Helmholtz-Institut Mainz and Institut für Kernphysik, J.Gutenberg-Universität Mainz, D-55099 Germany*

(Dated: November 11, 2016)

Abstract

There are excellent opportunities to produce excited heavy hyper residues in relativistic hadron and peripheral heavy-ion collisions. We investigate the disintegration of such residues into hyper nuclei via evaporation of baryons and light clusters and their fission. Previously these processes were well known for normal nuclei as the decay channels at low excitation energies. We have generalized these models for the case of hyper-matter. In this way we make extension of nuclear reaction studies at low temperature into the strange sector. We demonstrate how the new decay channels can be integrated in the whole disintegration process. Their importance for mass and isotope distributions of produced hyper-fragments is emphasized. New and exotic isotopes obtained within these processes may provide a unique opportunity for investigating hyperon interaction in nuclear matter.

PACS numbers: 25.75.-q , 21.80.+a , 25.70.Mn

I. INTRODUCTION

Hypernuclei are formed when hyperons ($Y = \Lambda, \Sigma, \Xi, \Omega$) produced in high-energy interactions are captured by nuclei. They live significantly longer than the typical reaction times. Baryons with strangeness embedded in the nuclear environment provide the only available possibility to approach the many-body aspect of the strong three-flavor interaction at low energies. In the same time, hypernuclei can serve as a tool to study the hyperon–nucleon and hyperon–hyperon interactions. The investigation of reactions leading to hypernuclei and the structure of hypernuclei is the progressing field of nuclear physics, because it provides complementary methods to improve traditional nuclear studies and open new horizons for studying particle physics and nuclear astrophysics (see, e.g., [1–6] and references therein).

Traditionaly for the hypernuclear physics focuses on spectroscopic information and is dominated by a quite limited set of lepton- and hadron-induced reactions [1, 3]. In these reactions the directly produced kaons are often used for tagging the production of hypernuclei in their ground and low excited states. However, very encouraging results on hypernuclei were obtained in experiments with relativistic ion collisions [7–9] and in other reactions where a large amount of energy is deposited in nuclei [10, 11]. Many experimental collaborations PANDA [12], CBM [13], HypHI, Super-FRS, R3B at GSI Facility for Antiproton and Ion reserach (FAIR) [14], BM@N and MPD at Nuclotron-based Ion Collider Facility (NICA) [15]) plan to investigate hypernuclei and their properties in reactions induced by relativistic hadrons and ions. The limits in isospin space, particle unstable states, multiple strange nuclei, and precision lifetime measurements are unique topics of these fragmentation reactions.

We especially emphasize a possibility to form hypernuclei in the deep-inelastic reactions leading to fragmentation processes, as they were discovered long ago [16]. As already discussed [5, 17], in these reactions initiated by high-energy hadrons, leptons, and ions one can get a very broad distribution of produced hypernuclei including the exotic ones and with the extreme isospin. This can help to investigate the structure of nuclei by extending the nuclear chart into the strangeness sector [1–3]. Complex multi hypernuclear systems incorporating more than two hyperons can be created in the energetic nucleus-nucleus collisions, and this may be the only conceivable method to go even beyond $|s| = 2$. An essential theoretical progress was achieved in the investigation of the normal nuclear reactions as-

sociated with both peripheral relativistic heavy-ion collisions and hadron-induced reactions (see, e.g., [18–21] and references therein). This gives us an opportunity to apply well known theoretical methods adopted for the description of these reactions also to the production of hypernuclei [22, 23]. In this paper we generalize the two very popular nuclear reaction models, the evaporation of light particles from the excited compound nucleus and the fission of the compound nucleus, for the description of the decay of excited hypernuclei. We investigate an important case of low excitation energies, in addition to high excitations leading to multifragmentation processes, which were analyzed previously in Refs. [5, 22]. As we show, many novel possibilities arise for formation of hypernuclei. New experiments on hypernuclei, in particular at GSI/FAIR and other accelerators, may be directed by employing such production mechanisms.

II. PRODUCTION OF EXCITED HYPER-RESIDUES

The hyperons are produced in high-energy particle reactions, e.g., nucleus-nucleus, hadron-nucleus and lepton-nucleus collisions. Usually, the emission of many particles accompanies the production of hyperons and an initial nucleus can lose many nucleons. As known from the interactions in normal nuclei, these processes will lead to a broad spectrum of excitations of remaining residual nuclei [19, 21]. For this reason the possibility to capture a hyperon will be realized mostly at an excited nucleus. We should note that a direct hyperon capture in the nuclear ground state has a very small probability. It is an important advantage of deep-inelastic processes that they allow for forming hyper-residues with very broad distribution in mass and excitation energy [17, 24].

The modifications in normal nuclei after the interaction with high energy hadrons and leptons are very well described in the literature (see, e.g., Ref. [18] and references therein). The production of strangeness is one of the possible channels and, besides the capture of few hyperons, we do not expect an essential change in the structure of a residue in this case. In comparison with hadron-induced reaction, the peripheral relativistic heavy-ion collisions lead to the larger number of individual nucleon-nucleon interactions and, as a result, to a larger number of produced particles related to a larger loss of nucleons from the residues. However, we have the same qualitative picture of what happens in the residues. As an example we refer to ion collisions in the following. It was demonstrated in the previous works [25, 26]

that the yields of the hypernuclear residues in peripheral ion collisions will saturate with energies above 3–5 A GeV (in the laboratory frame). Therefore, the accelerators of moderate relativistic energies can be used for the intensive studies of hypernuclei. The subthreshold production of hyperons becomes possible in these reactions down to the energies of $\sim$1 A GeV [24]. At the laboratory energies of ions around 1–2 A GeV one can effectively obtain nuclei with the modern experimental fragment separation methods [27–29]. This gives chances to measure many new exotic hypernuclei. Another research direction is related to increasing the energy up to $\sim$10 A GeV, when there is an opportunity to produce multistrange hyperfragments which can be measured with the high precision detectors, for example, by CBM collaboration at FAIR [13].

The typical excitation energies of the residues can be found from analysis of fragmentation/multifragmentation experimental data [18, 19, 21], as well as from the model calculations [24]. Both ways are consistent, and we have obtained the excitation energies from 0 to around 8 MeV per nucleon for these residues. The upper limit is naturally consistent with the nuclear binding energy, where the nuclei can still live for a time ($\sim$100 fm/c) sufficient for development of the collective decay modes (as multifragmentation). Because the hyperon life time in nuclei is essentially larger than the time for decay of excited nuclei, we must consider the de excitation processes leading to the production of really cold hypernuclei. As demonstrated previously, these processes are very promising for obtaining novel hypernuclei in the case of the multifragmentation break up at high excitation energy [5, 22]. In this paper we investigate the region of low excitation energies, where evaporation and fission decay modes dominate. Such excitations may be obtained in not-very-complicated reactions involving only few nucleons. For example, one nucleon can interact with an incident particle and be knocked out from a heavy nucleus. In addition, K^+ and a low-energy $\Lambda-$ hyperon may be produced. In the following K^+ can escape, and Λ may be captured inside the nucleus. In this case the background for hypernuclear experimental measurements is minimal. The "hole" in a nucleus from the nucleon can contribute with around 20 MeV (on average) to the nucleus excitation, whereas the hyperon capture may add another 10–20 MeV. In reality, however, the interactions with other nucleons may lead to more higher excitation energies. To describe the de excitation of low-excited hyper nuclei, we generalize the corresponding nuclear evaporation and fission models. We believe this generalization is possible because the hyperon-nucleon interaction is of the same order as the nucleon-nucleon one,

and the hyperon potential in a nucleus is considered as around 2/3 of the nucleon potential.

III. DE-EXCITATION OF HYPER-NUCLEI

For completeness, we provide knowledge about all main secondary de excitation processes, because they are complementary to each other. We expect the existence of hypernuclear decay mechanisms which are similar to the decay of normal nuclei.

A. Decay of light hyper-nuclei

We remind the reader that in the case of interaction with light nuclei ($A \lesssim 12-16$) the excited light hyper residues are produced after the dynamical stage. For their disintegration one can use the Fermi-break up model [18, 30] generalized by including Λ hyperons in Ref. [31]. In the microcanonical approximation we take into account all possible break up channels, which satisfy the mass number, hyperon number (i.e., strangeness), charge, energy, and momentum conservation and simulate the competition between these channels. The probability of each break up channel ch is proportional to the occupied phase space and the statistical weight of the channel containing n particles with masses m_i $(i = 1, \cdots, n)$ can be calculated as

$$W_{ch}^{mic} \propto \frac{S}{G}\left(\frac{V_f}{(2\pi\hbar)^3}\right)^{n-1}\left(\frac{\prod_{i=1}^{n} m_i}{m_0}\right)^{3/2} \cdot \frac{(2\pi)^{\frac{3}{2}(n-1)}}{\Gamma(\frac{3}{2}(n-1))} \cdot \left(E_{kin} - U_{ch}^{C}\right)^{\frac{3}{2}n-\frac{5}{2}}, \quad (1)$$

where $m_0 = \sum_{i=1}^{n} m_i$ is the summed mass of the particles, $S = \prod_{i=1}^{n}(2s_i+1)$ is the spin degeneracy factor (s_i is the i-th particle spin), $G = \prod_{j=1}^{k} n_j!$ is the particle identity factor (n_j is the number of particles of kind j). E_{kin} is the kinetic energy of nuclei and U_{ch}^{C} is the Coulomb interaction energy between nuclei, which are related to the energy balance as described in Ref. [31]. The table masses of both ground states and known excited states of (hyper-)nuclei (see, e.g., Refs. [1, 3]) are included. We have obtained in this case very encouraging predictions on the hypernuclei production [25, 31].

B. Sequential decay models: evaporation and fission

The successive particle emission from large hot primary nuclei is one of the basic de-excitation mechanism and it was implemented for the decay of normal compound nuclei nearly 60 yr ago [32]. This mechanism has been under intensive theoretical study and it is realized in many versions which provide very good descriptions of experimental data (e.g., see discussion in Ref. [18]). In this work we consider the generalization of the evaporation developed in Refs. [18, 30, 33–35], and extend it for hyper matter. For excited hyper-nuclei the modification of the standard evaporation scheme is the following: Besides emission of normal light particles (nucleons, d, t, α, and others up to oxygen) in ground and particle-stable excited states [30], we take into account the emission of strange particles (Λ-hyperon, ${}^{3}_{\Lambda}$H, ${}^{4}_{\Lambda}$H, ${}^{4}_{\Lambda}$He, ${}^{5}_{\Lambda}$He, and ${}^{6}_{\Lambda}$He). The width for the emission of a particle j from the compound nucleus (A, Z) is given by

$$\Gamma_j = \sum_{i=1}^{n} \int_0^{E^*_{AZ}-B_j-\epsilon_j^{(i)}} \frac{\mu_j g_j^{(i)}}{\pi^2\hbar^3}\sigma_j(E)\frac{\rho_{A'Z'}(E^*_{AZ}-B_j-E)}{\rho_{AZ}(E^*_{AZ})}EdE. \qquad (2)$$

Here the sum is taken over the ground and all particle-stable excited states $\epsilon_j^{(i)}$ ($i = 0, 1, \cdots, n$) of the fragment j, $g_j^{(i)} = (2s_j^{(i)} + 1)$ is the spin degeneracy factor of the ith excited state, μ_j and B_j are corresponding reduced mass and separation energy, E^*_{AZ} is the excitation energy of the initial (mother) nucleus, and E is the kinetic energy of an emitted particle in the center-of-mass frame. In Eq. (2) ρ_{AZ} and $\rho_{A'Z'}$ are the level densities of the initial (A, Z) and final (daughter) (A', Z') compound nuclei in the evaporation chain. The cross section $\sigma_j(E)$ of the inverse reaction $(A', Z') + j = (A, Z)$ was calculated using the optical model with nucleus-nucleus potential [30]. This evaporation process was simulated by the Monte Carlo method and the conservation of energy and momentum was strictly controlled in each emission step. After the analysis of experimental data we come to conclusion that at sufficient large excitation energies (more than 1 MeV per nucleon) it is reasonable to include the decreasing symmetry energy coefficient in mass formulas, which leads to adequate description of isotope distributions [33–35].

By considering the de excitation of hypernuclei we have taken into account their hyper energy term. In consistence with our previous works we suggest to use a reliable mass formula introduced in Ref. [5, 22], where the binding hyper energy $E_b^{\rm hyp}(A, H)$ is parametrized as

$$E_b^{\rm hyp}(A, H) = (H/A) \cdot (10.68A - 21.27A^{2/3})MeV. \qquad (3)$$

In this formula H is the hyperon number and the binding energy is proportional to the fraction of hyperons in the system (H/A). The second part represents the volume contribution reduced by the surface term and thus resembles the liquid-drop parametrization based on the saturation of the nuclear interaction. As demonstrated in Ref. [5] the formula gives a reasonable description of binding energies of known hypernuclei. A captured Λ-hyperon can occupy the s-state deep inside nuclei, because it is not forbidden by the Pauli principle. For this reason adding this hyperon to nuclei is a more effective way to increase their binding than adding nucleons, especially for large species. We apply the same formulas (2) for emission of hyperons and light hypernuclei, however, by taking into account that the additional hyper terms must appear in the corresponding separation energies B_j,

$$\Delta B_j = E_b^{\rm hyp}(A,H) - E_b^{\rm hyp}(A^{'},H^{'}), \tag{4}$$

where H and $H^{'}$ are the numbers of hyperons in mother and daughter nuclei, respectively. The hyper energy decreases also when the normal particles are emitted, In this case the additional hyper barrier is calculated with the same equation (4) by taking $H^{'} = H$. We have included the ground and the excited states of the hyper particles with their masses taken from the experimental tables [1, 3]. As in the case of the emission of normal particles [30] their masses explicitly enter the calculations of B_j. Presently we are interested in emission from the excited hyper residue containing one (or maximum two) absorbed hyperon. As follows from dynamical calculations [17], the capture of large numbers of hyperons is associated with more intensive collisions, which lead to higher excitation of residual nuclei; therefore, it comes up into another decay mode, e.g., multifragmentation (see below). Because the hyperon fraction is negligible in comparison with the total number of nucleons, we do not expect a considerable modification of the hyper nuclear properties as compared to the normal nuclear ones. In this case the level densities are taken as in the case of normal nuclei with the same mass number A. The inverse cross section is also taken as for reactions with normal nuclei by considering a neutron instead of a hyperon. We believe that all these approximations are sufficient for the first estimate of the evaporation of hyperons and light hyper clusters. However, it should be improved after obtaining more reliable data on hyperon-nucleon interaction and after the development of the advanced theoretical parametrizations. For the beginning we do not include the larger hyper particles with $A > 6$ for the emission in the model, because their probability will be essentially lower. However,

they (and their excited states) can be included within the described method too.

An important process of de excitation of heavy nuclei ($A \gtrsim 100$) is the fission of nuclei. This process competes with particle emission, and it can also be simulated with the Monte Carlo method at the each step of the evaporation-fission cascade. Following the Bohr-Wheeler statistical approach, we assume that the partial width for the normal compound nucleus fission is proportional to the level density at the saddle point $\rho_{sp}(E)$ [18],

$$\Gamma_f = \frac{1}{2\pi\rho_{AZ}(E^*_{AZ})} \int_0^{E^*_{AZ}-B_f} \rho_{sp}(E^*_{AZ} - B_f - E)dE, \tag{5}$$

where B_f is the height of the fission barrier, which is determined by the Myers-Swiatecki prescription. For approximation of ρ_{sp} we have used the results of the extensive analysis of nuclear fissility and Γ_n/Γ_f branching ratios; see Ref. [18] for details and references.

Similar to the evaporation case, we consider hypernuclei with a small number of absorbed hyperons (for the beginning H=1); therefore, we do not expect that the level density properties and the fission mechanism will change essentially in comparison with normal nuclei. The modification should concern the terms depending on the mass formulas because heavy hypernuclei are more strongly bound. For this reason the fission barrier for hypernuclei will be higher than that of normal nuclei. As a first approximation we assume that a hyper barrier B_f^{hyp} should be added in addition to the Myers-Swiatecki barriers. The final hyper energy release in the fission will be

$$E_0^{hyp} = E_b^{\rm hyp}(A, H) - E_b^{\rm hyp}(A', H). \tag{6}$$

Here A and A' are the mass numbers of the mother and daughter nuclei which contain a hyperon. However, because the barrier is determined in the saddle point, where nuclear fragments are not separated completely, B_f^{hyp} should be smaller than E_0^{hyp}. From our experience in normal fission we expect that the deformation of the surface at this point may take around one-half of the final value. So we assume that $B_f^{hyp} = E_0^{hyp}/2$. This is a quite conservative estimate which leads to increasing the fission barrier on about 0.5 MeV for heavy nuclei. There are other theoretical studies of the hypernuclei deformation [36] which tell us that the increasing the barrier, e.g., for ${}^{238}_{\Lambda}U$ may vary approximately from 0.2 to 0.8 MeV. We emphasize that such an increase is very small compared to the excitation energy of the hyper residues: Usually E^*_{AZ} is more than 10–20 MeV. This additional hyper barrier may slightly vary depending on masses of the formed fragments; however, the symmetric fission

is the most probable at high excitations. Therefore, we have adopted B_f^{hyp} at $A^{'} = A/2$ as a reasonable approximation for the calculation of the fission probability. We should take into account, of course, that for some specific nuclei at low excitation a more careful estimate of the fission barrier is necessary.

The mass distribution of the produced fission fragments is calculated similar to normal fission events; see Ref. [37]. Here we assume again that the small hyperon fraction cannot change the regularities established for normal nuclei, because the Λ-hyperon-nucleon interaction is qualitatively of the same order as nucleon-nucleon one. In this case a new uncertainty comes from the apparent deposition of the hyperon, in a bigger or a smaller fragment. We believe that it should be determined by the hyper binding energy, which is larger in a big fragment. The difference is

$$\Delta U^{hyp} = E_b^{\rm hyp}(A1, H) - E_b^{\rm hyp}(A2, H), \tag{7}$$

where $A1$ and $A2$ are masses of these fragments ($A = A1 + A2$). It is assumed that the probability $P1$ for the fragment $A1$ (if $A1 > A2$) to get a hyperon can be found in the canonical way,

$$P1 = 1/(1 + exp(-\Delta U^{hyp}/T)), \tag{8}$$

where $T = \sqrt{E^*_{AZ}/(aA)}$ is the temperature of the system, and $a \approx 0.125$ is the level density parameter. Because the both ΔU^{hyp} and T are of the order of MeV, this can lead to the essential redistribution of Λ-hyperons between big and small fragments.

The kinetic energy of the hyper fission fragments is generated as for normal fragments [18, 37] and depends only on their mass number and charge. After fission the separated fragments are still excited and evaporate few particles. We use the above-described version of the evaporation for the calculation of this process. As a result we obtain the cold fissioning remnants and several free particles in the end of the Monte Carlo simulation of each event.

All these models for secondary de excitation (evaporation and fission) were previously tested by numerical comparisons with experimental data on the decay of normal compound nuclei with excitation energies less than 2–3 MeV per nucleons [18, 30, 37]. For this reason we expect that our extension of these models should give reliable predictions for the preparation of future experiments.

C. Evolution from sequential decay to simultaneous break up

The concept of the compound nucleus cannot be applied at high excitation energies, $E^* \gtrsim 3$ MeV/nucleon with the corresponding temperature $T \gtrsim 5$ MeV. The reason is that the time intervals between subsequent fragment emissions, estimated both within the evaporation models [38] and from experimental data [39–42], become very short, on the order of a few tens of fm/c. In this case there will be not enough time for the residual nucleus to reach equilibrium between subsequent emissions. Moreover, the produced fragments will be in the vicinity of each other and, therefore, they should interact strongly. The rates of the particle emission calculated as in the case of isolated compound nuclei will not be reliable in this situation. There are many other theoretical arguments in favor of a simultaneous break up at high excitation energy. For example, the Hartree-Fock and Thomas-Fermi calculations predict that the compound nucleus will be unstable at high temperatures [43]. Sophisticated dynamical calculations have also shown that a nearly simultaneous break up into many fragments is the only possible way for the evolution of highly excited systems [44]. There also exist several analyses of experimental data which reject the binary decay mechanism of fragment production via sequential evaporation from a compound nucleus at high excitation energy [42, 45–47].

The picture of a simultaneous break up in some freeze-out volume is more justified at the high energy. Indeed, the time scales of less than 100 fm/c are extracted for multifragmentation reactions from experimental data [40, 41]. There are many experimental and theoretical works demonstrating a smooth transition from evaporation and fission modes to the fast multifragmentation break up of the whole nuclei with increasing excitation energy above 3 MeV/nucleon [18, 20, 37, 41, 42, 48, 49]. This break up can be described by the statistical laws, in particular, the statistical multifragmentation model (SMM) [18], where the disintegration channels are generated according to their statistical weight. The corresponding physics is related to the thermal expansion and density fluctuations of the nuclear matter. The SMM was previously generalized for hypernuclei in Ref. [22]: The grand canonical approximation leads to the following average yields of individual fragments:

$$Y_{\rm AZH} = g_{\rm AZH} V_f \frac{A^{3/2}}{\lambda_T^3} \exp\left[-\frac{1}{T}\left(F_{AZH}(T,V) - \mu_{AZH}\right)\right].$$
$$\mu_{AZH} = A\mu + Z\nu + H\xi, \qquad (9)$$

Here T is the temperature, $F_{AZH}(T)$ is the internal free energies of these fragments, V_f is the free volume available for the translation motion of the fragments in the freeze-out V, $g_{\rm AZH}$ is the ground-state degeneracy factor of species (A, Z, H), $\lambda_T = (2\pi\hbar^2/m_N T)^{1/2}$ is the nucleon thermal wavelength, and m_N is the average nucleon mass. The chemical potentials μ, ν, and ξ are responsible for the mass (baryon) number, charge, and strangeness conservation in the system. A transition from the compound hyper-nucleus to multifragmentation regime has already been demonstrated [5, 22]. The combination of all de-excitation modes in a universal hypernuclear model (as it was done in SMM [18]) will be a subject of our forthcoming works.

IV. DISCUSSION OF THE RESULTS

In the beginning it is important to demonstrate that different de-excitation mechanisms (evaporation, fission and multifragmentation) are connected with each other in the real disintegration process. In Figs. 1 and 2 we show how the mass distributions of produced fragments evolve with the excitation energy of the ^{209}Bi source. These calculations are performed only for normal nuclei. One can see that at low excitations (1 MeV per nucleon) we have standard evaporation and fission fragments. With increasing excitation energy the channels of multifragmentation decay responsible for producing intermediate mass fragments come into force. Already at 2.5 MeV per nucleon a considerable part of fragments with A>15 are produced in the fast multifragmentation break up. As was mentioned, we expect qualitatively the same evolution for hypernuclear systems too.

The probabilities of the evaporation and fission processes can be easily measured in experiments. They are often used for testing the corresponding models. In Figs. 3 and 4 we demonstrate the evolution of these probabilities for heavy nuclei with their excitation energy. In particular, the "fission" means that the nuclei undergo fission during the de excitation at one of the steps of the evaporation-fission cascade. The label "evaporation residue" means that only evaporation of nucleons and light clusters take place during the de-excitation without fission. As one can see from calculations for normal nuclei (Fig. 3) the fission occurs certainly for very big nuclei (^{238}U) and it is strongly suppressed for medium-heavy nuclei (^{165}Ho). In the same time the fission probability of medium-heavy nuclei increases with excitation energy essentially. Actually, it is consistent with the past experiments. For the big nuclei in between we can have obvious competition among these decay channels (^{209}Bi),

and this can be measured in experiments too. We have shown this figure to facilitate the understanding the next Fig. 4, where the same processes are presented for evaporation and fission taking place in hyper nuclei.

For all nuclear systems shown in Fig. 4 one Λ-hyperon is implemented in nuclei instead of one neutron. The single hypernuclei will be the most probable case in nuclear reaction, especially with deposition of low excitation energy [24]. The capture of many hyperons is usually accompanied by large nucleon loses, and, therefore, should lead to high excitation energies which are typical for multifragmentation channels [22, 35]. In Fig. 4 one can see similar trends for the fission and evaporation-residue probabilities as in Fig. 3. However, in this case one of the "hyper-fission" remnants will have a hyperon. Otherwise, the residue after evaporation (noted as "evap. Λ –residue") can contain this Λ hyperon. Another important channel shown in the Fig. 4 is the probability of the Λ-hyperon evaporation. One can see that this probability increases with excitation energy; however, it remains essentially smaller than the dominating process probability. It is because the Λ binding energy keeps this hyperon inside the nuclei.

As was discussed above, besides the evaporation of Λ, an evaporation of light hyper-clusters is also possible from the excited hyper-compound. It is demonstrated in Fig. 5 for ${}^{3}_{\Lambda}$H, ${}^{4}_{\Lambda}$H, ${}^{4}_{\Lambda}$He, ${}^{5}_{\Lambda}$He, and ${}^{6}_{\Lambda}$He hyper-nuclei. Similar to the single Λ evaporation the yield of these hyper nuclei increases considerably with increasing excitation energy. Still, the yield of these hypernuclei is essentially less than Λ-hyperons (more than one order of magnitude), and the probabilities of dominating evaporation/fission processes are much higher (compare Fig. 5 with Fig. 4). Evaporation of light clusters is well known in normal nuclear reactions. In the case of investigation of hypernuclei these processes may play a very important role, because they are produced as a result of a complex collective phenomena, but not as a result of a direct (or a coalescence-like) process in a final state. Previously, indications for existing of the unusual ΛNN state coming from the disintegration of the excited projectile residues were reported [50]. They were never observed in direct reactions. This gives an opportunity to study how the formation of hypernuclei in new exotic states depends on the reaction mechanism. The lightest hypernuclei can be reliably identified in the projectile/target kinematic region by the decay correlation between the pions and normal fragments. As our calculations show (Fig. 5), the emission of ${}^{5}_{\Lambda}$He has largest probability, because of its considerable binding energy. As one can also see from the emulsion experiments

[51], these hypernuclei have the largest yield in comparison with others.

Now we would like to draw more attention to the details of the hyper-fission process. As is well known, during the time of the deformation to the fission saddle point the compound nucleus can lose particles and the excitation energy via evaporation. Therefore, the nuclear composition at the saddle will be different than that in the beginning of the evaporation-fission cascade. We have plotted this effect in Figs. 6 and 7 depending on the excitation energy for the ${}^{209}_{\Lambda}$Bi case. The symbol "hot" corresponds to the parameters at the saddle point after which the fission process can become irreversible. The symbol "cold" presents the average parameters of fission remnants after their scission and final evaporation cascade. The statistical deviations obtained in the Monte-Carlo simulations are shown by the 'error bars' separately above and below from the average values. We see that the initial nucleus can loose around ten nucleons during its evolution to the saddle deformation, and this pre-saddle emission increases with the excitation energy (Fig. 6). In addition the nucleus may lose a considerable part of the available energy (fig. 7). However, it is interesting that the fission barrier at the saddle can first decrease slightly at low excitations. This is because neutron are mainly evaporated, which increases the fissility. At high excitations, since many protons are evaporated also, the fissility decreases and the barrier becomes higher. Some residual excitation is predicted for the "cold" remnants and this excitation can be taken away by γ emission. It may be used for examining hypernuclear structure too.

The typical characteristic for the fission process is the mass distribution of the fission fragments. In Figs. 8 and 9 we show the evolution of these mass distributions with excitation energy for fissioning ${}^{238}_{\Lambda}$U and ${}^{209}_{\Lambda}$Bi hypernuclei. As for the normal nuclear matter [18, 37] the uranium fission leads to the mixture of the asymmetric and symmetric modes at low excitation energy [Fig. 8(a)], which turn into the symmetric fission at more high excitations [Figs. 8(a) and (b)]. There are also small additions from the compound nucleus evaporation without fission. For the intermediate-heavy hypernuclei (Bi, Fig. 9) we expect only the symmetric fission with the considerable contribution from the compound nucleus evaporation. Both the evaporation and fission mass distributions become wider with the excitation. Note that in these figures we have presented the hyper-fragments only (i.e., they contain a Λ-hyperon). The complementary fission remnant is a normal fragment. Therefore, we can see in these figures slightly non-symmetric fission distributions, because the hyperons remain with greater probability in the largest fragments [see formula (8)]. It is especially

obvious from panel (a) of Fig. 8, where the yield in the right asymmetric mode is higher than that in the left one. Previously, a similar distribution of hyperons between the remnants was reported in experiment [10].

Recently, the fission and evaporation processes in normal nuclei were discussed in the context of obtaining new nuclear isotopes. This is related to extending the nuclear chart and investigating the structure of exotic nuclei. We emphasize that involving hypernuclei provides novel opportunities for this research; see, e.g., discussion in our previous works [5, 22]. In Figs. 10–13 we demonstrate the isotope composition of hypernuclei produced as a results of evaporation-fission cascade. Actually, we calculate the probabilities of obtaining the isotopes in the case of de excitation initial U, Bi, and Sn hypernuclei at different excitation energies. The presentation of the results in the charge-neutron number plane is convenient for the overview and the selection of what reaction can be better for studying the specific isotopes.

The results in Figs. 10 and 11 are obtained for two heavy fissioning nuclei, uranium and bismuth, which can capture a hyperon. Right above, at big charges close to the initial one, we see the region of the compound hyper residues after the evaporation decay. As expected, there are large neutron losses during the evaporation, which can be seen clear in comparison with the domain of the stable nuclei shown in the figures too. For the low excitation energy (0.25 MeV per nucleon) one can obtain a lot of intermediate neutron-rich hypernuclei as a result of the fission process. For normal nuclei, namely the fission reaction is considered as the promising method for obtaining the exotic neutron-rich nuclei. The presence of hyperons inside nuclei can increase their binding energy and we can get even a more exotic nuclear species [5]. With increasing excitation energy the subsequent de-excitation leads to neutron-poor hypernuclei, which would be also interesting for further studies. The general trends of the fragment yield after fissioning are qualitatively the same for both the heavy nuclei.

A promising nuclear method used in recent years is the comparative measurements for similar nuclei, however, with very different isospin. In our opinion, one of the important applications of newly obtained hypernuclear isotopes should be the studies of their lifetimes. It is known that the lifetime of Λ-hyperons inside nuclei is different from the lifetime of free Λ [52]. This is related to the subtle effects of weak interaction within nuclear matter. By producing neutron-rich and neutron-poor hypernuclei one can make a critical examination of the influence of nuclear isospin on the hyperon decay time. For this purpose one can use

neutron-rich (-poor) projectiles (or targets) in relativistic ion collisions, that are possible to realize, e.g., at the GSI/FAIR facility [28, 29]. For this reason in Figs. 12 and 13 we show the yield probabilities of hyper-elements coming after disintegration of tin hypernuclei with essentially different isospin content. By comparing ${}^{124}_{\Lambda}$Sn and ${}^{112}_{\Lambda}$Sn cases we see that the corresponding regions of final cold hypernuclei are well separated. In particular, the production of neutron-rich and neutron-poor hypernuclei does clear correlate with the initial isotope composition. In comparison with usual hypernuclear reactions, the procedure of the lifetime measurements is quite simple in the case of relativistic ions [52]. Therefore, we think valuable information on the isospin dependence may be obtained rather soon in such experiments.

V. CONCLUSION

The disintegration processes well established for excited normal nuclei can take place in hot hypernuclei also. It gives an opportunity to investigate the evolution of strange matter in such nuclei at relatively low temperature and obtain various hypernuclear states. Because the hyperon interaction within the matter is of the same order as the nucleon one, the extension of the reaction models designed for de excitation of normal nuclei becomes possible for hypernuclei. In this work we have developed the models of the particle evaporation and the fission for excited hypernuclei. The critical ingredient which has to be included in the model is the binding energy of hyperons inside nuclei.

We demonstrate that the results of hypernuclear evaporation and fission apparently taking place in deep inelastic nuclear collisions look similar to normal evaporation and fission processes. However, final hypernuclei obtained in this case offer a new direction for investigation. This may concern the production of exotic states which can exist because of the presence of a hyperon. It will be difficult to obtain such a state in other reactions, in particular, because there are practical limitations for using radioactive targets in experiments. We show the evaporational mechanism for emission of light hypernuclei which takes place from the target-projectile residues. Namely, the collective processes are responsible for formation of these small and large clusters. Therefore, contrary to phenomena of final state interactions for coalescence like and direct processes, novel hypernuclear states may be realized in this case. Important theoretical predictions are related to the fission process,

which can be responsible for very neutron-rich hypernuclei. These nuclei can be used for many purposes, for example, by aiming at approaching the neutron-star conditions: There is a special interest in finding the weak decay lifetime dependence versus isospin. One can also extract the isospin dependence of the hyperon binding energy in neutron-rich matter via the comparison of the hypernuclei yields.

The extension of the nuclear reaction research by involving captured hyperons will certainly have an impact on the field. It is a big advantage that in these reactions we obtain a very broad distribution of hypernuclei, as one can see from the calculated nuclear charts. Such nuclei can be immediately (on line) used for the extensive studies of their unknown properties.

Acknowledgments

A.S. Botvina acknowledges the support of BMBF (Germany). N.B., A.E., and R.O. acknowledge the TUBITAK support under Project No. 114F328. N.B. and R.O. thank the Frankfurt Institute for Advanced Studies (FIAS), J.W. Goethe University for hospitality during the research visits.

---

[1] H. Bando, T. Mottle, and J. Zofka, Int. J. Mod. Phys. **A5**, 4021 (1990).

[2] J. Schaffner, C.B. Dover, A. Gal, C. Greiner, and H. Stoecker, Phys. Rev. Lett. **71**, 1328 (1993).

[3] O. Hashimoto, H. Tamura, Prog. Part. Nucl. Phys. **57**, 564 (2006).

[4] A. Gal, O Hashimoto and J. Pochodzalla (Edt.), Special issue on *Progress in Strangeness Nuclear Physics*, Nucl. Phys. A **881**, 1-338 (2012).

[5] N. Buyukcizmeci, A.S. Botvina, J. Pochodzalla, and M. Bleicher, Phys. Rev. C **88**, 014611 (2013).

[6] T. Hell and W. Weise, Phys. Rev. C **90**, 045801 (2014).

[7] The STAR collaboration, Science **328**, 58 (2010).

[8] B. Dönigus *et al.* (ALICE collaboration), Nucl. Phys. A**904-905**, 547c (2013).

[9] T.R. Saito *et al.* (HypHI collaboration), Nucl. Phys. A **881**, 218 (2012).

[10] T.A. Armstrong, J.P. Bocquet,G. Ericsson, T. Johansson, T. Krogulski, R.A. Lewis, F. Malek, M. Maurel, E. Monnand, J. Mougey, H. Nifenecker, J. Passaneau, P. Perrin, S.M. Polikanov,M. Rey-Campagnolle, C. Ristori, G.A. Smith, G. Tibell, Phys. Rev. C **47**, 1957 (1993).

[11] H. Ohm, T. Hermes, W. Borgs, H.R. Koch, R. Maier, D. Prasuhn, H.J. Stein, O.W.B. Schult, K. Pysz, Z. Rudy, L. Jarczyk, B. Kamys, P. Kulessa, A. Strzalkowski, W. Cassing, Y. Uozumi, I. Zychor,Phys. Rev. C **55**, 3062 (1997).

[12] The PANDA collaboration, http://www-panda.gsi.de ; and arXiv:physics/0701090.

[13] I. Vassiliev for CBM collaboration. Hypernuclei program at the CBM experiment. HYP2015, http://indico2.riken.jp/indico/contributionListDisplay.py?confId=2002

[14] https://indico.gsi.de/event/superfrs3 (access to pdf files via timetable and key 'walldorf').

[15] NICA White Paper, http://theor.jinr.ru/twiki-cgi/view/NICA/WebHome ; http://nica.jinr.ru/files/BM@N .

[16] M. Danysz and J. Pniewski, Philos. Mag. **44**, 348 (1953).

[17] A.S. Botvina, K.K. Gudima, J. Steinheimer, M. Bleicher, I.N. Mishustin, Phys. Rev. C **84**, 064904 (2011).

[18] J.P. Bondorf, A.S. Botvina, A.S. Iljinov, I.N. Mishustin, and K. Sneppen, Phys. Rep. **257**, 133 (1995).

[19] H. Xi *et al.*, Z. Phys. A **359**, 397 (1997).

[20] R.P. Scharenberg, B.K. Srivastava, S. Albergo,F. Bieser, F.P. Brady, Z. Caccia,D.A. Cebra, A.D. Chacon, J.L. Chance, Y. Choi, S. Costa, J.B. Elliott, M.L. Gilkes, J.A. Hauger, A.S. Hirsch, E.L. Hjort, A. Insolia, M. Justice, D. Keane, J.C. Kintner, V. Lindenstruth, M.A. Lisa, H.S. Matis, M. McMahan, C. McParland, W.F.J. Muller, D.L. Olson, M.D. Partlan, N.T. Porile, R. Potenza, G. Rai,J. Rasmussen, H.G. Ritter, J. Romanski,J.L. Romero,G.V. Russo, H. Sann, A. Scott,Y. Shao, T.J.M. Symons, M. Tincknell, C. Tuve, S. Wang, P. Warren, H.H. Wieman, T. Wienold, K. Wolf, Phys. Rev. C **64**, 054602 (2001).

[21] R. Ogul *et al.*, Phys. Rev. C **83**, 024608 (2011).

[22] A.S. Botvina and J. Pochodzalla, Phys. Rev. C **76**, 024909 (2007).

[23] S.Das Gupta, Nucl. Phys. A **822**, 41 (2009).

[24] A.S. Botvina, K.K. Gudima, J. Steinheimer, M. Bleicher, J. Pochodzalla , arXiv:1608.05680v1 , 2016.

[25] A.S. Botvina, K.K. Gudima, J. Pochodzalla, Phys. Rev. C **88**, 054605 (2013).

[26] A.S. Botvina *et al.*, Phys. Lett. B **742**, 7 (2015).

[27] C.Rappold, T.R. Saito, and C. Scheidenberger. Simulation Study of the Production of Exotic Hypernuclei at the Super-FRS (at GSI Scientific report 2012), GSI Report 2013-1, 176 p. (2013). http://repository.gsi.de/record/52079 .

[28] Th. Aumann, Progr. Part. Nucl. Phys. **59**, 3 (2007).

[29] H. Geissel *et al.*, Nucl. Inst. Meth. Phys. Res. B **204**, 71 (2003).

[30] A.S. Botvina et al., Nucl. Phys. **A475**, 663 (1987).

[31] A.S. Lorente, A.S. Botvina, and J. Pochodzalla, Phys. Lett. B **697**, 222 (2011).

[32] W. Weisskopf, Phys. Rev. **52**, 295 (1937).

[33] N. Buyukcizmeci, R. Ogul, A.S. Botvina, Eur. Phys. J. A **25**, 57 (2005).

[34] D. Henzlova, A.S. Botvina, K-H. Schmidt *et al.*, J. Phys. G **37**, 085010 (2010).

[35] H. Imal, A. Ergun, N. Buyukcizmeci, R. Ogul, A.S. Botvina, W. Trautmann, Phys. Rev. C **91**, 034605 (2015).

[36] F. Minato, S. Chibo, K. Hagino, Nucl. Phys. A **831**, 150 (2009).

[37] N. Eren *et al.*, Eur. Phys. J. A **49**, (2013) 48.

[38] R.J. Charity, Phys. Rev. **C61**, 054614 (2000).

[39] M. Jandel et al., J. Phys. **G: 31**, 29 (2005).

[40] L. Beaulieu, T. Lefort, K. Kwiatkowski, R.T. deSouza,W.-c. Hsi, L. Pienkowski, B. Back, D.S. Bracken, H. Breuer, E. Cornell, F. Gimeno-Nogues, D.S. Ginger, S. Gushue, R.G. Korteling, R. Laforest, E. Martin, K.B. Morley, E. Ramakrishnan, L.P. Remsberg, D. Rowland, A. Ruangma, V.E. Viola, G. Wang,E. Winchester, S.J. Yennello, Phys. Rev. Lett. **84**, 5971 (2000).

[41] V.A. Karnaukhov et al., Phys. Atom. Nucl. **66** 1242 (2003).

[42] L. Pienkowski, K. Kwiatkowski, T. Lefort, W.-c.Hsi, L. Beaulieu,V.E. Viola, A. Botvina, R.G. Korteling, R. Laforest, E. Martin, E. Ramakrishnan, D. Rowland, A. Ruangma, E. Winchester, S. J. Yennello, B. Back, S. Gushue, L.P. Remsberg, Phys. Rev. **C65**, 064606 (2002).

[43] P. Bonche, S. Levit, and D. Vautherin, Nucl. Phys. **A436**, 265 (1985). E. Suraud, Nucl. Phys. **A462**, 109 (1987).

[44] S. DasGupta, C. Gale, J. Gallego, H.H. Gan, R.D. RatnaRaju, Phys. Rev. **C35**, 556 (1987). B.J. Strack, Phys. Rev. **C35**, 691 (1987). D.H. Boal, J.N. Glosli, Phys. Rev. **C37**, 91 (1988).

[45] J. Hubele, P. Kreutz, V. Lindenstruth, J.C. Adloff, M. Begemann-Blaich, P. Bouissou, G.

Imme, I. Iori,G.J. Kunde, S. Leray, Z. Liu, U. Lynen,R.J. Meijer,U. Milkau, A. Moroni, W.F.J. Muller, C. Ngo, C.A. Ogilvie, J. Pochodzalla, G. Raciti,G. Rudolf, H. Sann, A. Schuttauf, W. Seidel, L. Stuttge, W. Trautmann, A. Tucholski, R. Heck, A.R. DeAngelis, D.H.E. Gross, H.R. Jaqaman, H.W. Barz, H. Schulz, W.A. Friedman, R.J. Charity, Phys. Rev. **C46**, R1577 (1992).

[46] P. Desesquelles et al., Nucl. Phys. **A604**, 183 (1996).

[47] P. Napolitani, K.H. Schmidt, A.S. Botvina, F. Rejmund, L. Tassan-Got, C. Villagrasa, Phys. Rev. **C70**, 054607 (2004).

[48] A.S. Botvina et al., Nucl. Phys. A **584**, 737 (1995).

[49] M. D'Agostino et al., Nucl. Phys. A **650**, 329 (1999).

[50] C. Rappold, et al., Phys. Rev. C **88**, 041001 (R) (2013).

[51] D. H. Davis, Contemp. Phys. **27**, 91 (1986).

[52] C. Rappold, T.R. Saito, et al., Phys. Lett. B **728**, 543 (2014).

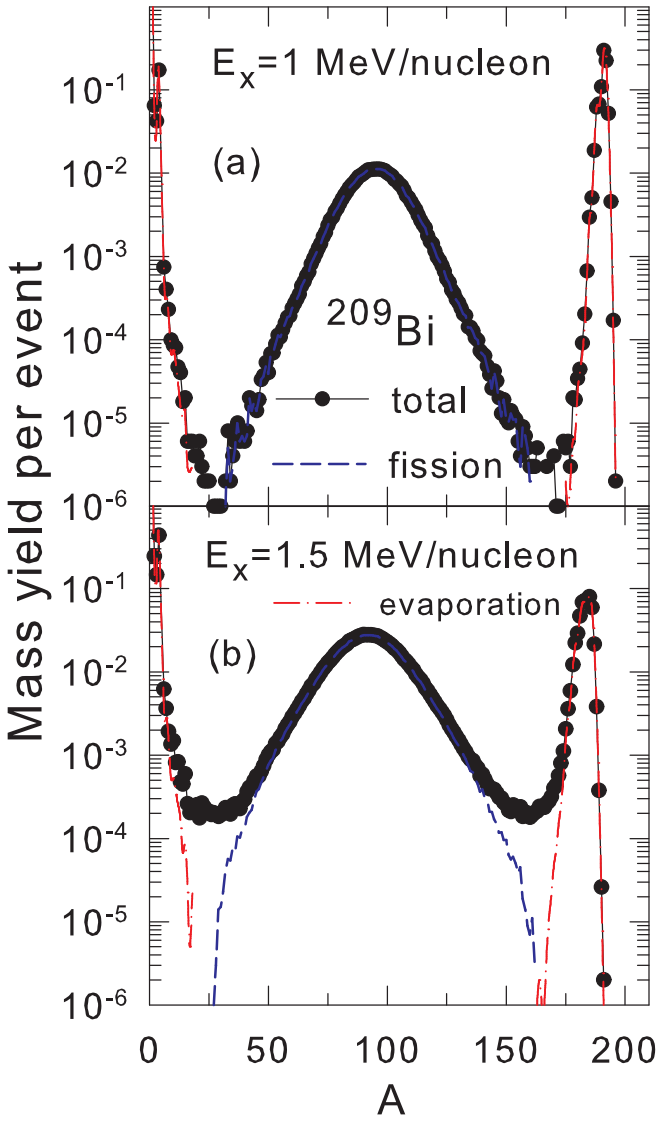

FIG. 1: (Color online) Fragment mass distributions produced after disintegration of ^{209}Bi excited normal nuclear systems. Excitation energies are given in panels (a), (b), and (c). The calculations include all decay processes for heavy nuclei: The contributions of fission (dashed blue lines) and evaporation (red dot-dashed lines) of the initial compound nuclei are shown separately. The rest to the total yields (solid lines with black circles) belong to the contribution of multifragmentation process.

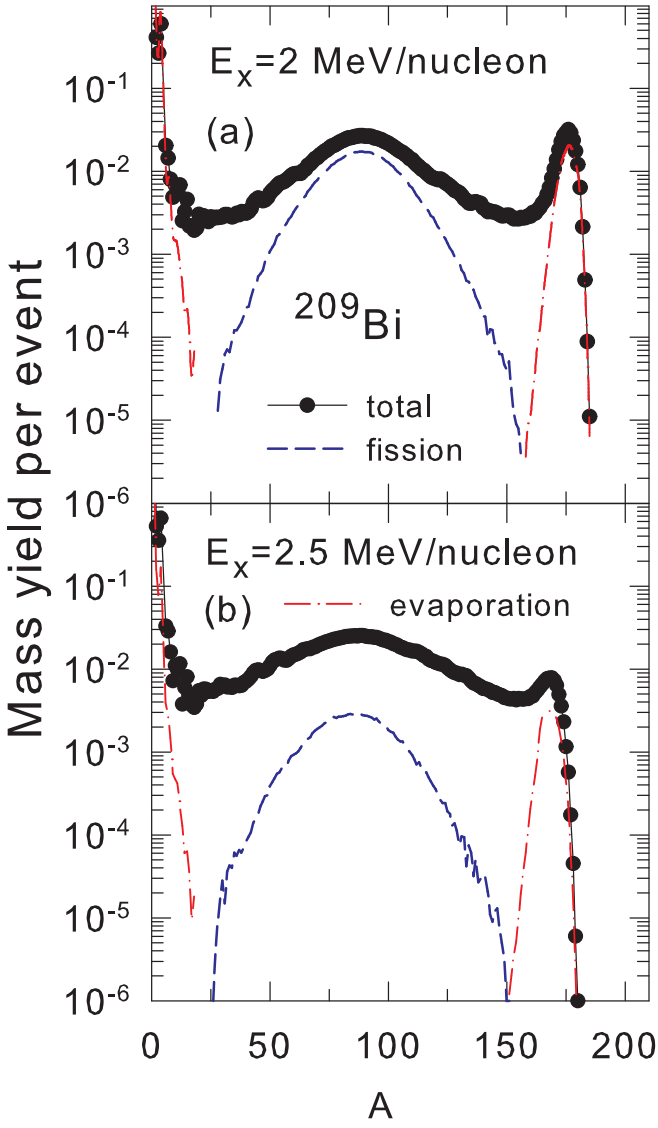

FIG. 2: (Color online) The same as in Fig. 1 but for higher excitation energies.

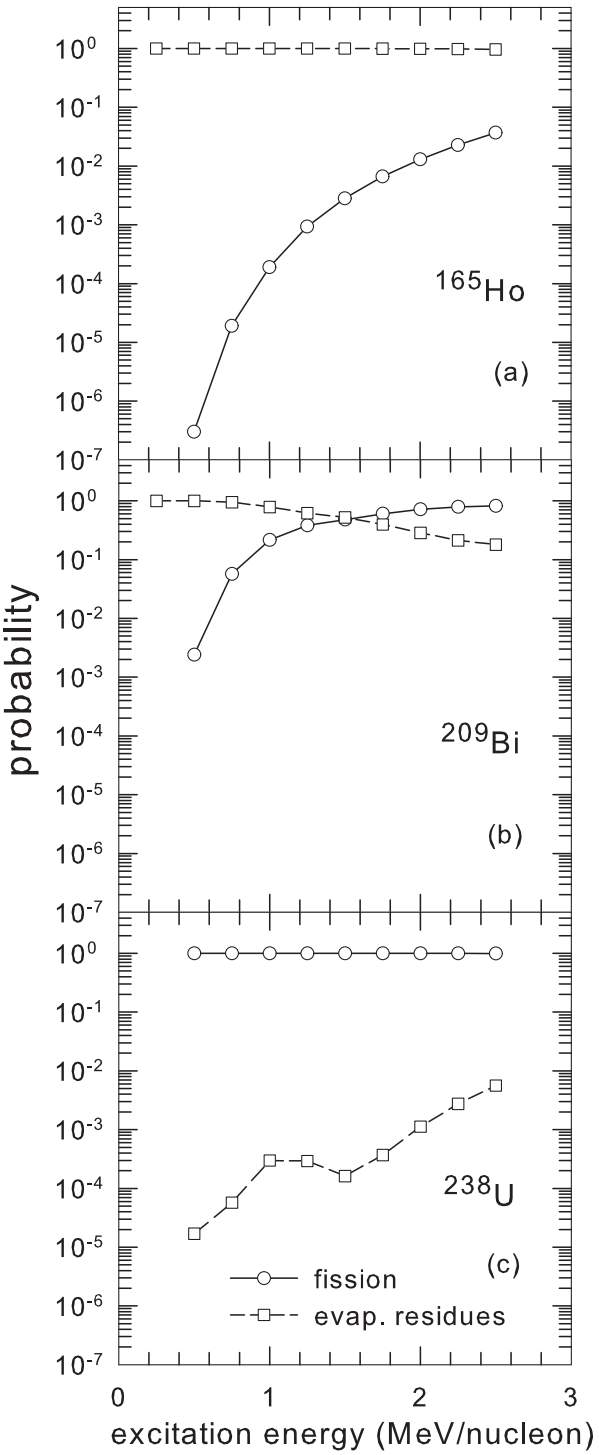

FIG. 3: Probability of the nuclear fission (circles, solid lines) and surviving the compound nucleus after evaporation of light particles (squares, dashed lines) versus excitation energy of nuclei. The nuclei are noted at the panels (a), (b), and (c).

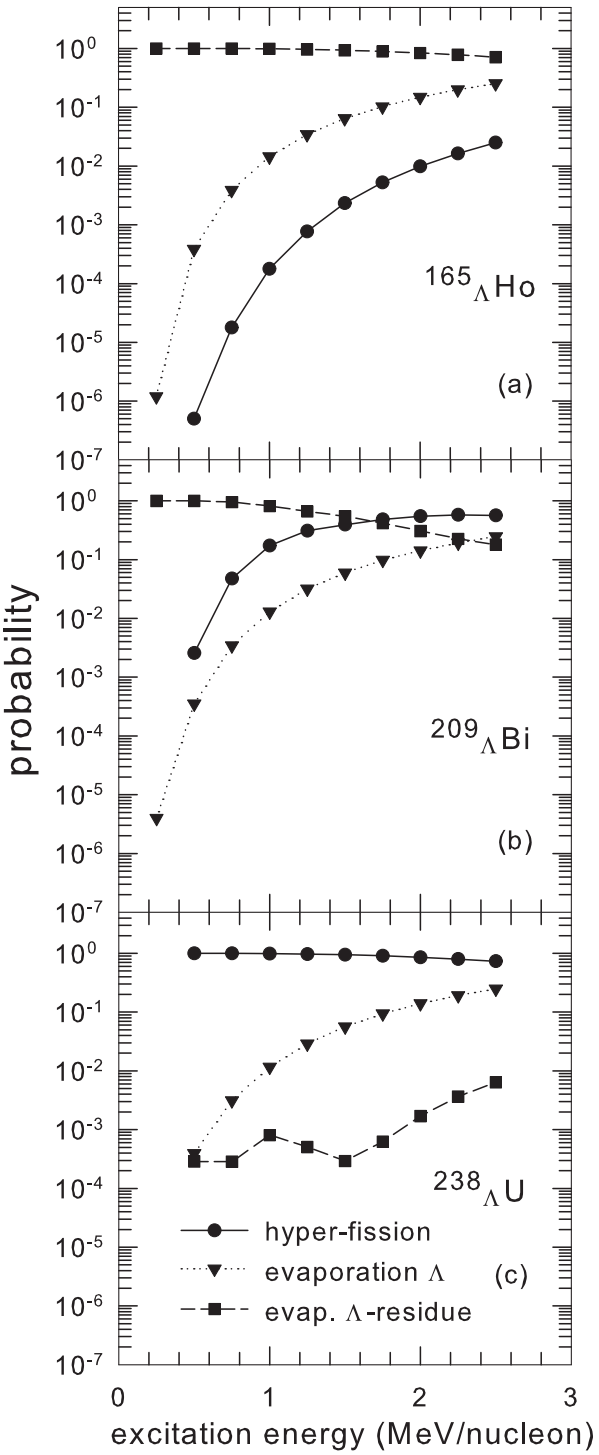

FIG. 4: Probability of the hyper-nuclear fission (solid circles, solid lines) and surviving the compound hyper-nucleus after evaporation of light particles (solid squares, dashed lines) versus excitation energy of hyper-nuclei. The solid triangles (dotted lines) give the probability for emission of single Λ-hyperons. The initial compound hyper-nuclei are noted in panels (a), (b), and (c).

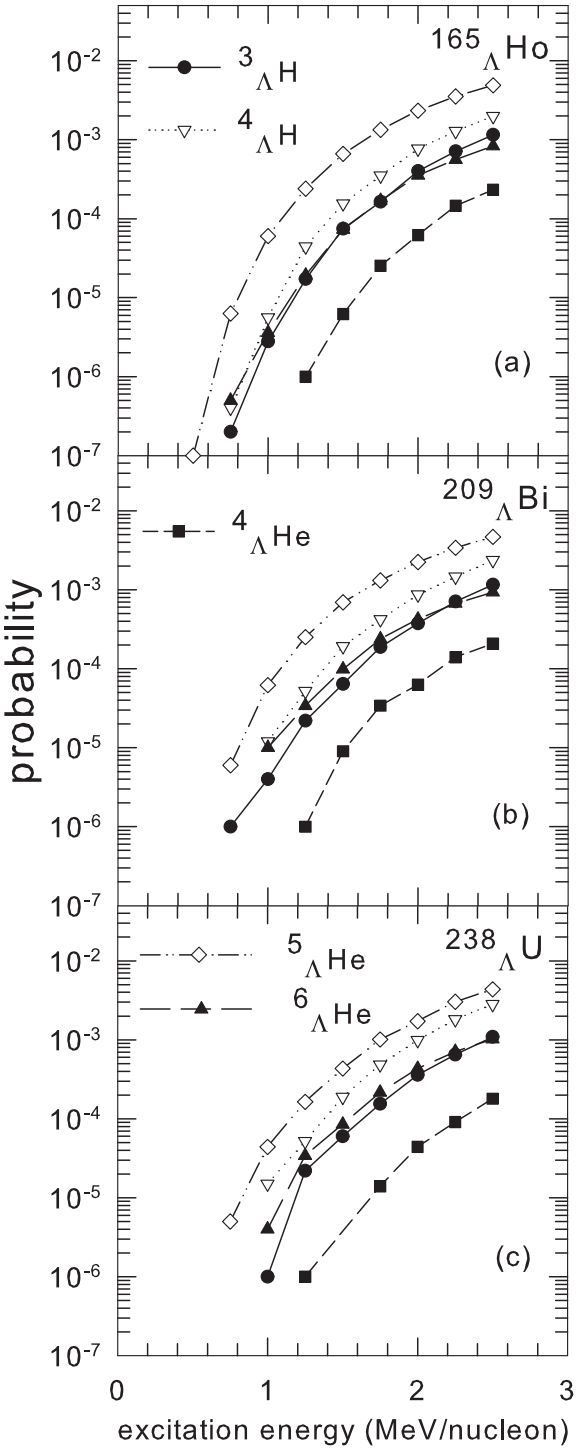

FIG. 5: Probability of the evaporation of light hyper-nuclei from heavy compound hyper-nuclei (see panels) versus excitation energy. The notations for evaporated nuclei (symbols and lines) are given in panels (a), (b), and (c).

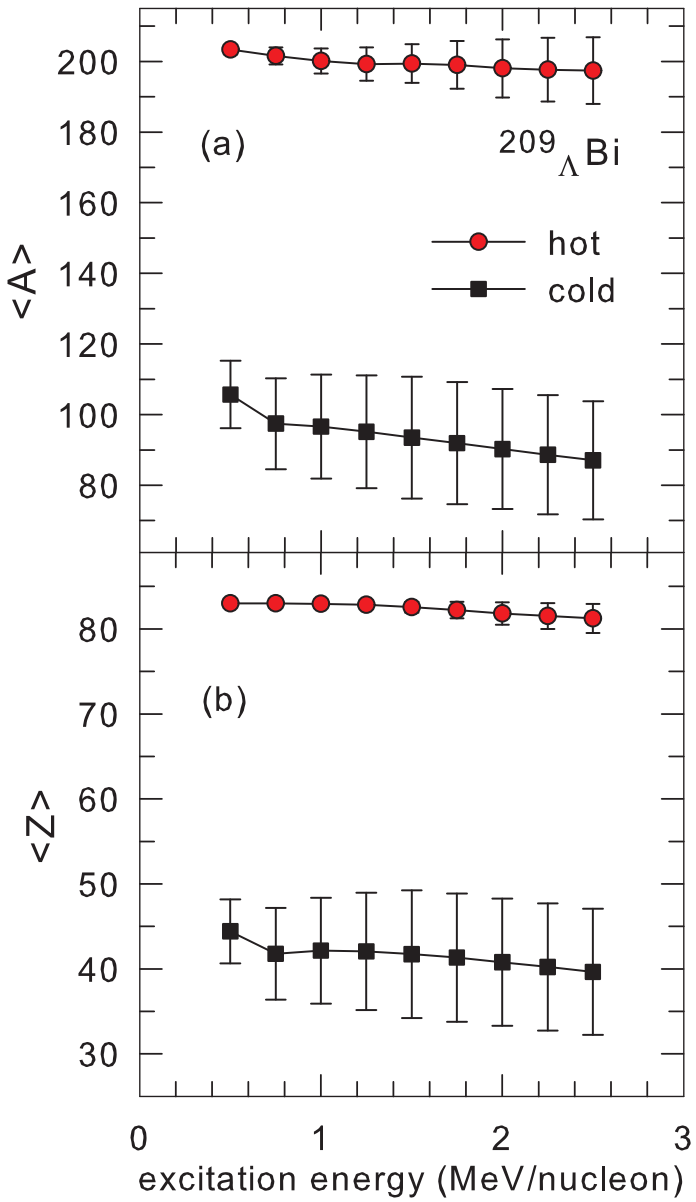

FIG. 6: (Color online) Average mass numbers [top panel (a)] and charges [bottom panel (b)] for the fissioning $^{209}_{\Lambda}$Bi hyper-nuclei at the saddle point (noted as hot, red circles), and for final nuclear remnants after their de excitation (noted as cold, black squares), versus the excitation energy. The statistical deviations are shown by error bars.

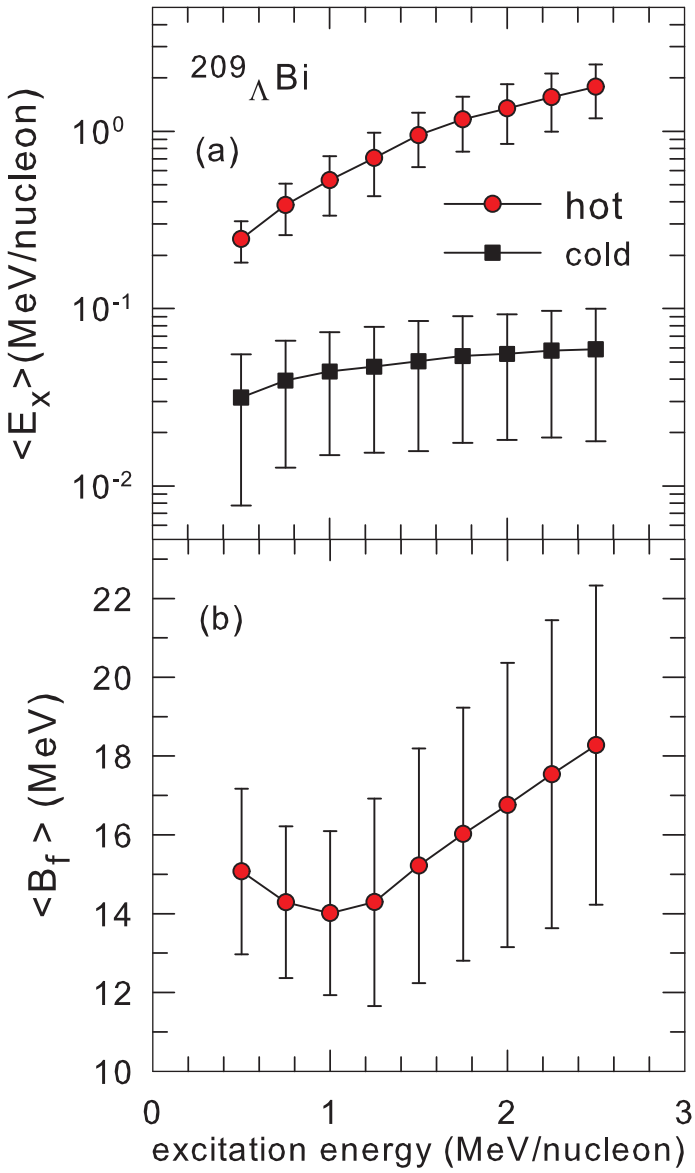

FIG. 7: (Color online) The average excitation energy [E^* (a)] and the fission barrier [B_f (b)] of the fissioning $^{209}_{\Lambda}$Bi hyper nuclei at the saddle point (noted as hot) versus initial excitation energy. The remaining excitation energy of fission remnants is given on the panel (a) too. Other notations are as in Fig. 6.

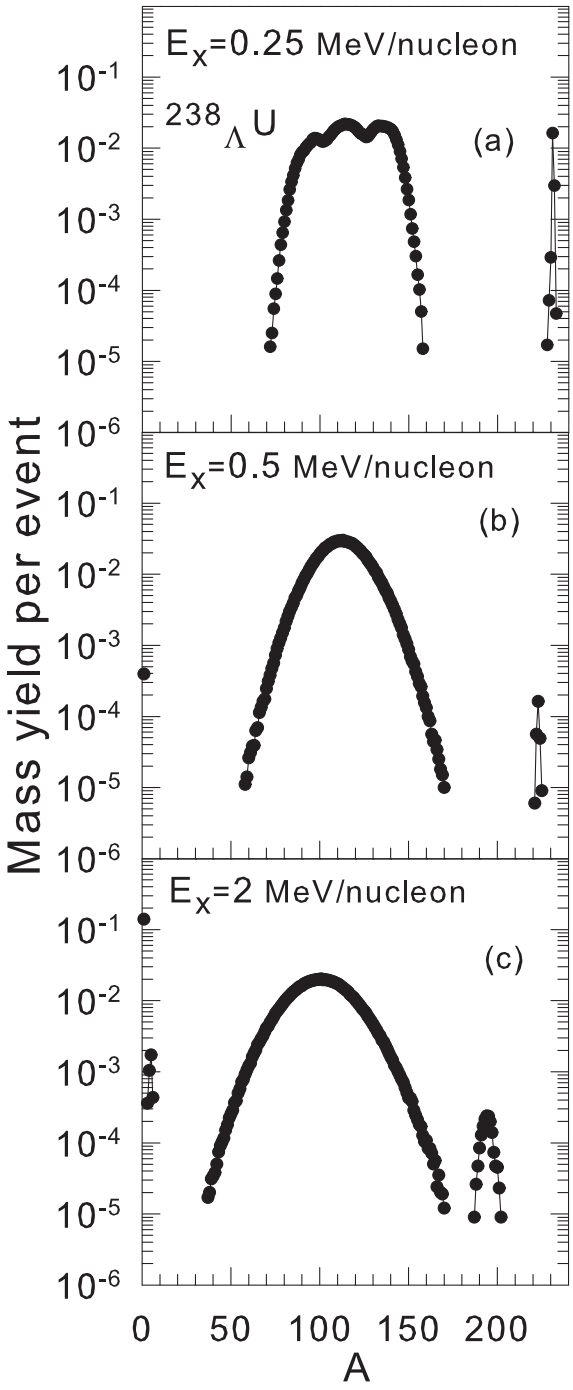

FIG. 8: Mass distributions of fission and evaporation hyper-fragments after disintegration of ${}^{238}_{\Lambda}$U hypernuclei at different excitation energies E_x [in MeV per nucleon; see panels (a), (b), and (c)]. The calculations include the competition of evaporation and fission decay modes.

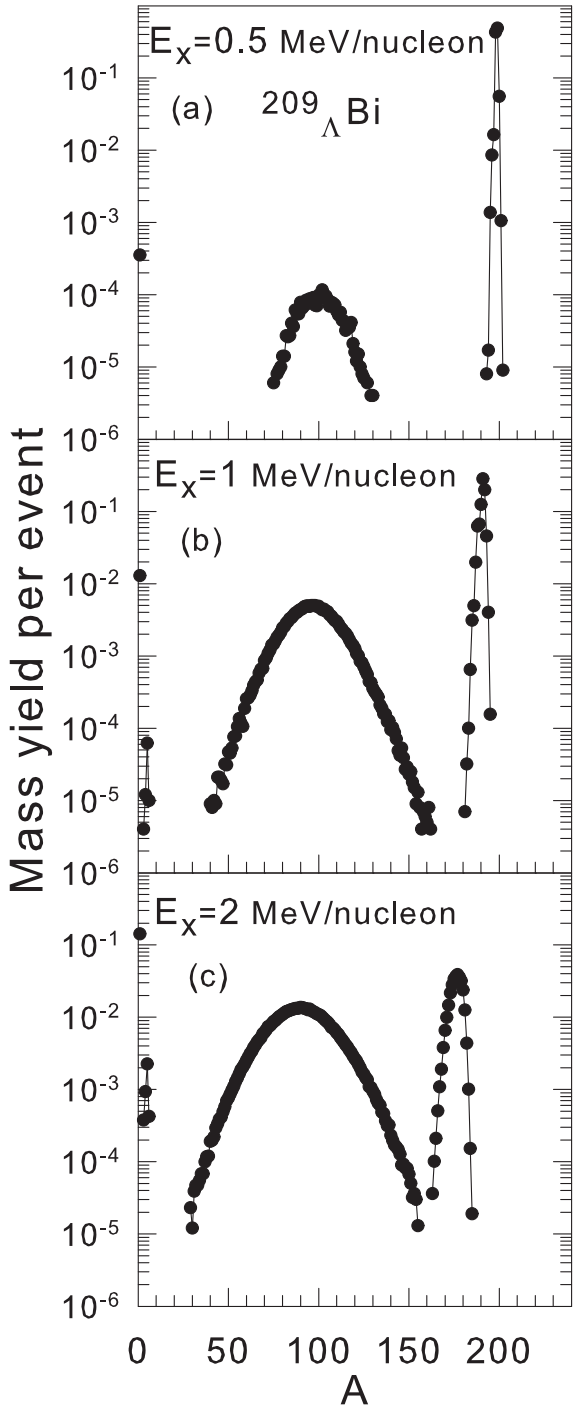

FIG. 9: The same as in Fig. 8, however, for $^{209}_{\Lambda}$Bi excited hypernuclei.

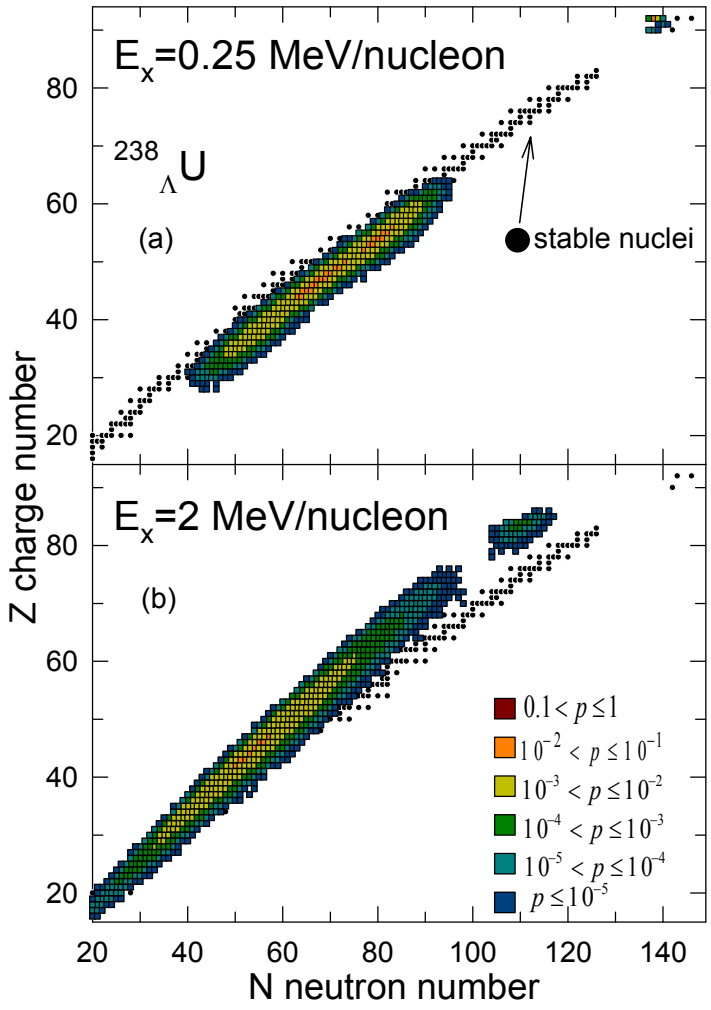

FIG. 10: (Color online) Probabilities of the yield (normalized per one event) of single hypernuclei produced after evaporation and fission of the excited initial $^{238}_{\Lambda}$U hypernucleus. The squares present the nuclei in the plane of the charge number (Z) neutron number (N). The location of stable normal nuclei (from the nuclear chart) are represented by the dark circles to facilitate the comparison. Colors of the squares corresponding to the calculated ranges of the probability p of these hypernuclei are given in the figure. Excitation energies are noted in panels (a) and (b).

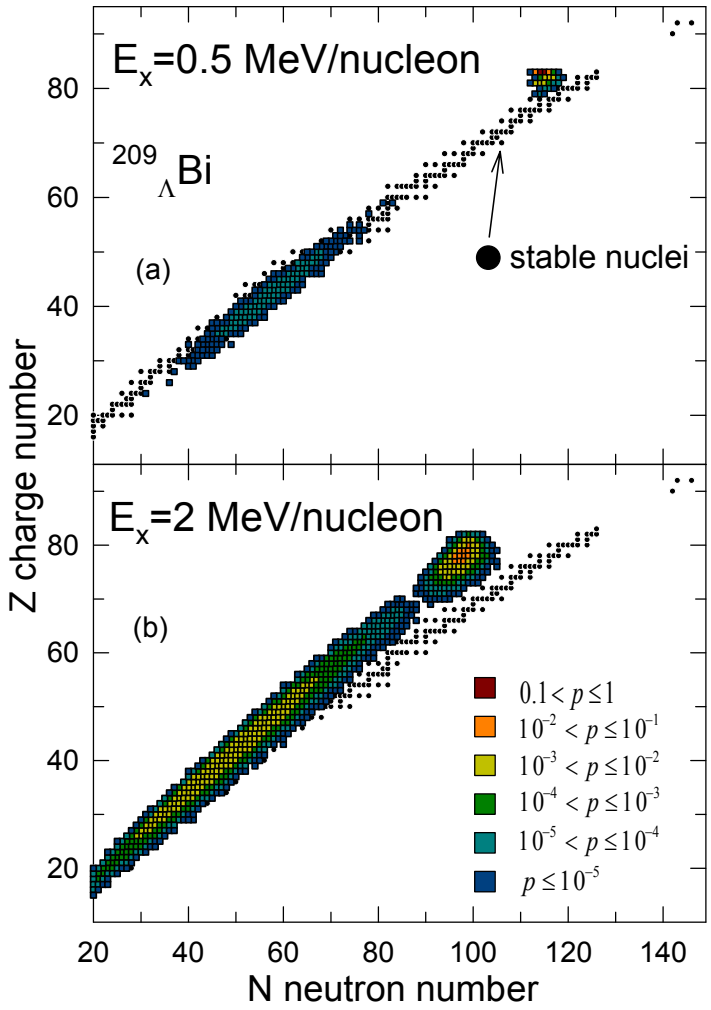

FIG. 11: (Color online) The same as in Fig. 10, however, for the initial ${}^{209}_{\Lambda}$Bi hypernucleus.

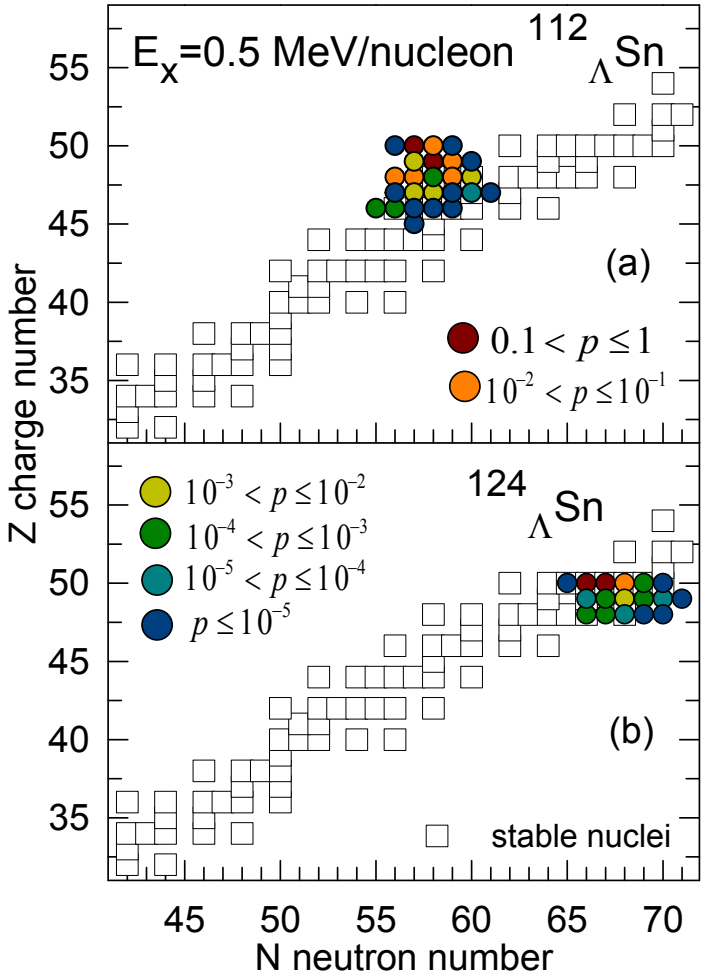

FIG. 12: (Color online) Probabilities of the yield (normalized per one event) of single hypernuclei produced after evaporation and fission of the excited initial ${}^{112}_{\Lambda}$Sn (a) and ${}^{124}_{\Lambda}$Sn (b) hypernucleus at the excitation energy 0.5 MeV per nucleon. The circles present the nuclei in the plane of the charge number (Z) neutron number (N). The location of stable normal nuclei (from the nuclear chart) are represented by the empty squares. Colors of the circles corresponding to the calculated ranges of the probability p of these hypernuclei are given in the figure.

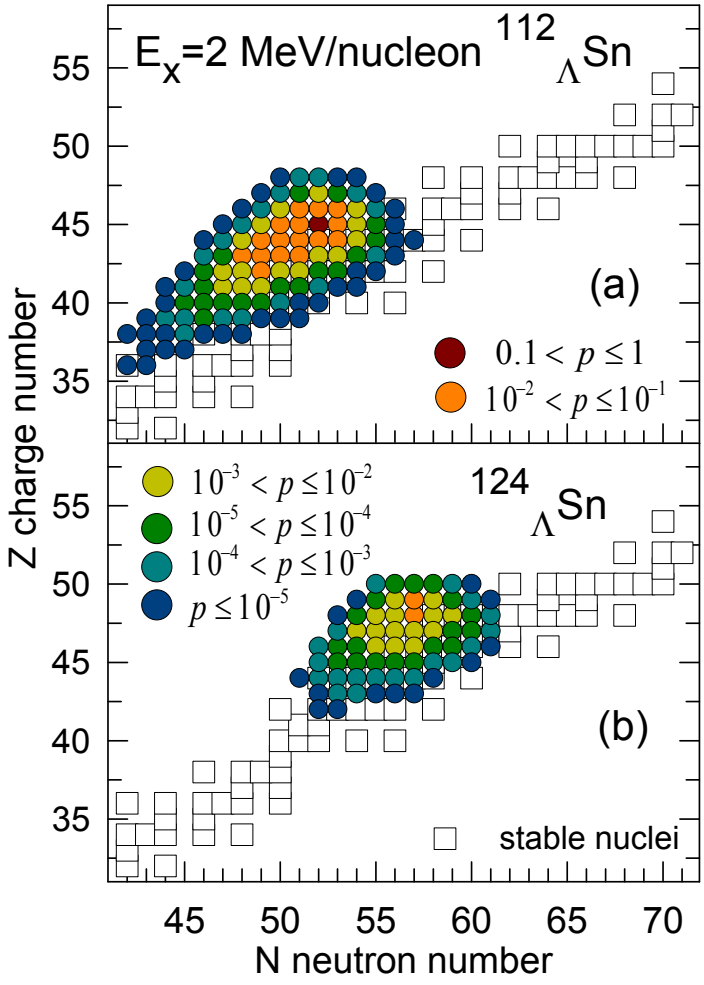

FIG. 13: (Color online) The same as in Fig. 12, however, for the excitation energy 2 MeV per nucleon.